Self-consistent calculation of the polarizability of small jellium spheres

D. E. Beck
Department of Physics and Laboratory for Surface Studies, University of Wisconsin—Milwaukee, Milwaukee, Wisconsin 53201
(Received 29 May 1984)

A self-consistent, density-functional calculation of the static polarizability of small metal spheres is reported. The jellium model of a metal, in which the positive ions are replaced by a uniform positive background, is employed, and the modified Sternheimer equation is used to compute the static dipole polarizability. The computations are reported for the closed-shell configurations containing from 8 to 254 electrons for neutral and charged spheres.

I. INTRODUCTION

Recently a number of self-consistent field calculations of the polarizability of atoms[1–3] have been reported. These calculations utilize the density-functional formalism and employ the random-phase-approximation (RPA) to provide an, in principle, exact calculation of the static polarizability. Mahan[2] recast this calculation in terms of the Sternheimer equation for the calculation of the polarizability of atoms,[4] and his modified equation permits a straightforward calculation of the multipole polarizability of closed-shell ions. The jellium model for small metal spheres,[5,6] where the positive ions of the metal are replaced by a uniform sphere of positive charge and the valence electrons are treated self-consistently using the Kohn-Sham[7,8] procedure, fits quite naturally into this formalism, and we report here a self-consistent calculation of the static dipole polarization for these spheres.

A variational calculation of the static polarizability of this model for a metal sphere has recently been reported by Snider and Sorbello.[9] However, they use a gradient expansion to compute the kinetic energy, so the electrons are not treated wave mechanically in their calculation. Ekardt[10] has performed a self-consistent random-phase-approximation (RPA) calculation of the polarizability of these spheres, and, since the modified Sternheimer equation is fully equivalent to the RPA calculation[2] there is some overlap between his results and those reported in this paper. Rice, Schneider, and Strässler[11] have also reported an RPA calculation, but they use the wave functions for an electron confined in a sphere by an infinite barrier which severely limits the ability of the electrons to respond to a perturbing field.[12]

Our quantum-mechanical, self-consistent calculations of the dipole polarizability of neutral and charged spheres containing from 8 to 254 electrons are reported in Sec. III of this paper. Comparisons with the other calculations discussed above and with density-functional calculation for the response of a flat metal surface to an applied electric field[13,14] are also given in this section, and Sec. IV contains a summary of the conclusions we can draw from these data. The formalism used in the calculation is set forth in Sec. II. We have provided only a brief discussion of the formalism in this section and placed a number of the details in Appendix A. Appendix B contains a brief outline of the numerical procedures used in the calculation.

II. FORMALISM

If a spherically symmetric electronic system is subjected to an infinitesimal external, multipole potential of the form

$$\delta V_M(\vec{r})=r^M Y_M^0(\hat{r})\epsilon_M ,$$

it will develop a moment

$$p_M=\alpha_M\epsilon_M$$

in response to the applied field. Here α_M is the Mth-order polarizability and $Y_l^m(\hat{r})$ is a spherical harmonic.

The first-order response of the ground-state system to this perturbing field is described by an infinitesimal change in the electronic wave functions,

$$\psi_i(\vec{r})\rightarrow\psi_i(\vec{r})+\epsilon_M\phi_i(\vec{r})$$

and the corresponding change in the density

$$n(\vec{r})=\sum_{i=1}^{N}|\psi_i(\vec{r})|^2\rightarrow n(\vec{r})+\epsilon_M\delta n(\vec{r}) , \tag{1}$$

where

$$\delta n(\vec{r})=2\mathrm{Re}\left[\sum_{i=1}^{N}\psi_i^*(\vec{r})\phi_i(\vec{r})\right] . \tag{2}$$

We use the density-functional formalism[5,7] to compute the properties of the ground-state system, and the energy of the electrons for the unperturbed system is given by

$$E[n]=\int d\vec{r}\,v(\vec{r})n(\vec{r})+\tfrac{1}{2}\int d\vec{r}\int d\vec{r}'\frac{n(\vec{r})n(\vec{r}')}{|\vec{r}-\vec{r}'|}$$
$$+T_s[n]+\int d\vec{r}\,\epsilon_{xc}[n]n(\vec{r}) .$$

Here the exchange-correlation energy is approximated by a local-density expression, $\epsilon_{xc}(\vec{r})$:

$$\epsilon_x[n]=-\frac{3}{4}\left[\frac{3n}{\pi}\right]^{1/3} ,$$

for the exchange, and the Wigner's interpolation formula for the correlation,

$$\epsilon_c[n]=-\frac{0.44}{(3/4\pi n)^{1/3}+7.8}$$

(we use atomic units, $e=\hbar=m=1$, throughout this paper; the length unit is the Bohr radius and the energy unit is 27.2 eV). The external potential $v(\vec{r})$ is provided by a uniform positive sphere of charge $n_+(\vec{r})=n_0$ for $r\leq R$.

The Kohn-Sham[8] procedure is used to obtain a set of self-consistent, noninteracting single particle wave functions, $\psi_i(\vec{r})$, for the N-electron system. These wave functions satisfy the Schrödinger equation

$$(-\tfrac{1}{2}\nabla^2+v_{\rm eff}[n;\vec{r}])\psi_i(\vec{r})=\epsilon_i\psi_i(\vec{r}) , \tag{3}$$

where the effective potential is given by

$$v_{\rm eff}[n;\vec{r}]=v(\vec{r})+\int d\vec{r}'\frac{n(\vec{r}')}{|\vec{r}-\vec{r}'|}+\frac{d}{dn}(n\epsilon_{\rm xc}[n]) , \tag{4}$$

and the kinetic energy of the system is given by

$$T_s[n]=\sum_{i=1}^{N}\langle\psi_i|(-\tfrac{1}{2}\nabla^2)|\psi_i\rangle .$$

Self-consistency requires that one obtains a set of wave functions consistent with Eqs. (1), (3), and (4), and this model for the electron density was the subject of earlier papers.[5,6]

Using first-order perturbation theory and the Schrödinger equation (3), one easily obtains an equation for the change in the wave functions, ϕ_i, when the perturbing field is present,

$$(-\tfrac{1}{2}\nabla^2+v_{\rm eff}[n;\vec{r}]-\epsilon_i)\phi_i(\vec{r})=-v_{\rm SCF}[\delta n;\vec{r}]\psi_i(\vec{r}) , \tag{5}$$

where the self-consistent field is given by

$$v_{\rm SCF}[\delta n;\vec{r}]=r^M Y_M^0(\hat{r})+\int d\vec{r}'\frac{\delta n(\vec{r}')}{|\vec{r}-\vec{r}'|}+\delta n(\vec{r})\frac{\partial^2}{\partial n^2}(n\epsilon_{\rm xc}[n]) . \tag{6}$$

This is the modified Sternheimer equation obtained by Mahan.[2]

The calculation of the polarizability proceeds by obtaining a self-consistent set of wave functions, $\psi_i(\vec{r})$, and eigenvalues, ϵ_i, for the field-free system and then solving the modified Sternheimer equation (5) to obtain a self-consistent set of functions, $\phi_i(\vec{r})$. Using these, one computes $\delta n(\vec{r})$, Eq. (2), and obtains the polarizability

$$\alpha_M=\int d\vec{r}\,r^M Y_M^{0*}(\hat{r})\delta n(\vec{r}) .$$

Mahan[2] proves that for closed shell (spherically symmetric) systems the only nonzero terms in the expansions of $\delta n(\vec{r})$ and $v_{\rm SCF}[\delta n;\vec{r}]$ in spherical harmonics are those with the same symmetry as the perturbation,

$$\delta n(\vec{r})=\sum_L \delta n_L(r)Y_L^0(\hat{r})=\delta n_M(r)Y_M^0(\hat{r}) \tag{7}$$

and

$$v_{\rm SCF}[\delta n;\vec{r}]=v_M[\delta n;r]Y_M^0(\hat{r})$$

where

$$v_M[\delta n;r]=r^M+\frac{4\pi}{2M+1}\int dr'(r')^2\delta n_M(r')\frac{r_<^M}{r_>^{M+1}}+\delta n_M(r)\frac{\partial^2}{\partial n^2}(n\epsilon_{\rm xc}[n]) . \tag{8}$$

Furthermore, he demonstrates that for a particular linear combination of the angular functions only the radial part of the inhomogeneous equation for $\phi_i(\vec{r})$, Eq. (5), needs to be solved. A shortened but lucid proof of these results is set forth in Appendix A.

For a spherically symmetric potential, $v_{\rm eff}[n;r]$, we can write

$$\psi_i(\vec{r})=r^l u_{nl}(r)Y_l^m(\hat{r})$$

where the ith orbital has quantum numbers ($nlms$). The functions $u_{nl}(r)$ are eigenfunctions of the second-order differential operator L_l,

$$L_l u_{nl}=\epsilon_{nl}u_{nl}(r) \tag{9}$$

with

$$L_l=-\frac{1}{2}\frac{d^2}{dr^2}-\frac{l+1}{r}\frac{d}{dr}+v_{\rm eff}[n;r] . \tag{10}$$

In Appendix A we demonstrate that the perturbed density, Eq. (2), is given by

$$\delta n_M(r)=(2s+1)2\,{\rm Re}\left[\sum_{n,l,l'} r^l u_{nl}^*(r)r^{l'}\times\bar{u}_{nl,l'}(r)c(M;l,l')\right] . \tag{11}$$

The factor $2s+1=2$ accounts for the spin degeneracy, and the numerical coefficients $c(M;l,l')$, Eq. (A5), are those evaluated by Mahan.[2] They are expressed in terms of Clebsch-Gordon coefficients in Appendix A. The radial functions $\bar{u}_{nl,l'}(r)$, Eq. (A4), are obtained by expressing $\phi_i(\vec{r})$ in terms of spherical harmonics, and they satisfy the radial part of the modified Sternheimer equation (5),

$$(L_{l'}-\epsilon_{nl})\bar{u}_{nl,l'}(r)=-v_M[\delta n;r]r^{l-l'}u_{nl}(r) . \tag{12}$$

The polarizability is given by

$$\alpha_M=\frac{4\pi}{2M+1}\int_0^\infty dr\,r^{M+2}\delta n_M(r) . \tag{13}$$

The differential equations for $u_{nl}(r)$ and $\bar{u}_{nl,l'}(r)$ are converted into matrix equations by introducing a set of quadrature points r_j and converting the differential operator L_l into a finite-difference expression. The eigenvectors and eigenvalues of the matrix equation for $u_{\ln}(r_j)$ are determined numerically and the inhomogeneous equation for $\bar{u}_{nl,l'}(r_j)$ is solved by numerically inverting the matrix. The interested reader is referred to Appendix B, where details of the numerical procedures are outlined.

Only the calculation for the static dipole polarizability

($M=1$) is reported in this paper, since it describes the linear response of a spherical metal particle placed in a uniform electric field. A check on the overall accuracy of the numerical procedures for this calculation is provided by the sum rule for the electrostatic force on the positive background of an isolated neutral object in a uniform external field.[15] The most convenient form for the sum rule for this check is the statement that the electrostatic potential due to the external field and the induced charge distribution should vanish at the surface of the sphere containing the positive charge. This potential is just the first two terms in the expression for $v_M[\delta n;r]$, Eq. (8), and, equating these terms to zero for a sphere of radius R, we obtain

$$\frac{4\pi}{3}\left[\frac{1}{R^3}\int_0^R dr\, r^3\delta n_1(r)+\int_R^\infty dr\,\delta n_1(r)\right]=-\frac{N_-}{N_+}\ . \quad (14)$$

Here we have replaced -1 by $-N_-/N_+$ which expresses the sum rule for a system with positive charge eN_+ and negative charge eN_-.[16,17]

III. RESULTS

The static, dipole polarization is computed for jellium spheres with $r_s=(3/4\pi n_0)^{1/3}$ values of 2.00 and 4.00 a.u. The calculations are reported for neutral spheres and charged spheres having one extra electronic charge, $\pm e$. The results for closed-shell configurations containing from 8 to 254 electrons are shown in the figures. Since the classical dipole polarizability of a metal sphere of radius R is $\alpha_{\rm cl}=R^3$, a convenient representation of the polarization data is provided by the parameter

$$\delta=\alpha_1^{1/3}-R\ . \quad (15)$$

Snider and Sorbello[9] argue that in the limit as $R\to\infty$, this quantity coincides with the centroid of the induced electron density for a flat surface, δ_p. This centroid has been computed by Lang and Kohn[13,14] for the same model of a metal that we employ. Their values for δ_p are indicated on Fig. 1 along with our calculated values for neutral spheres [for $r_s=2.00$, $\delta_p=1.6\pm0.05$; for $r_s=4.00$, $\delta_p=1.3\pm0.2$ (Ref. 14)].

The points in the figures are labeled with the quantum numbers (nl) denoting the highest filled level (those points with two sets of numbers have a second filled level with an energy near that of the highest filled level). Because of the degeneracy of the high angular-momentum orbitals $N_l=2(2l+1)$ and the asymptotic behavior of the wave functions, $\psi_i(\vec{r})\propto r^{-1}\exp[-r(-2\epsilon_{nl})^{1/2}]$, the filling of the states with $n=1$ strongly influences the portion of the electronic density which extends outside of the positive background charge. This part of the density is seen to govern the response of the system to the perturbing field as illustrated in Fig. 2, where $\alpha_1/\alpha_{\rm cl}$ is plotted versus the fraction of the electronic charge outside of the sphere of radius R for the field-free system,[5] $\Delta N/N$, where

$$\Delta N=4\pi\int_R^\infty dr\, r^2 n(r)\ . \quad (16)$$

This presentation of our data also facilitates a comparison with the variational calculation[9] for these spheres and

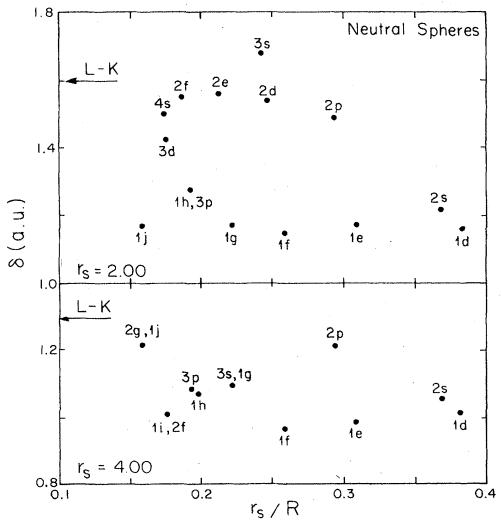

FIG. 1. Polarizability parameter δ for neutral spheres. The data are for the closed-shell configurations where the sphere contains from 18 to 254 electrons. The computed points are labeled by the quantum numbers (nl) denoting the filled level with the highest energy (a second set of numbers denote a second filled level whose energy is very near that of the highest level). The arrows, labeled L-K, denote the flat surface values for δ_p from Ref. 14.

the calculations for plane metal surfaces.[14] In the limit as $R\to\infty$,

$$\alpha_1/\alpha_{\rm cl}\approx 1+3(\delta/R)$$

and

$$\Delta N\approx(3N/R)\int_R^\infty dr[n(r)/n_0]\ ,$$

since $n(r)$ decreases rapidly outside of the sphere. Hence, we have

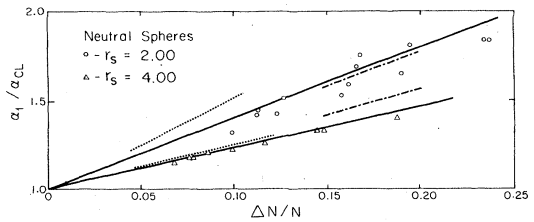

FIG. 2. Static dipole polarization enhancement $\alpha_1/\alpha_{\rm cl}$, where $\alpha_{\rm cl}=R^3$ and R^3 is the radius of the sphere containing the uniform positive charge, versus the fraction of the electronic charge $\Delta N/N$ outside of the sphere of radius R in the field-free calculation, Ref. 5. The points are computed for the same configurations reported in Fig. 1 and an additional sphere with $r_s=4.00$ containing eight electrons. The solid lines are drawn with slopes determined from the plane surface calculations of Ref. 14 using Eq. (17). The other lines in the figure have slopes determined from the variational calculation of Ref. 9, again using Eq. (17) ($R=40$ a.u.): dotted-dashed lines are for a gradient expansion parameter of $\frac{1}{36}$; dotted lines for a gradient expansion parameter of $\frac{1}{72}$.

$$\lim_{R\to\infty}(\alpha_1-\alpha_{cl})N/\alpha_{cl}\Delta N=\delta_p\Big/\int_0^\infty dz[n_p(z)/n_0]\ , \qquad (17)$$

where δ_p and $n_p(z)$ are the quantities for a plane metal surface (the integral is over the electron density extending beyond the edge of the uniform positive background located at $z=0$). The slopes of the solid lines in Fig. 2 are determined by this expression.[14] The dotted and dotted-dashed lines in the figure have slopes corresponding to the values of this ratio obtained from the variational calculation ($R=40$ a.u.].[9]

For $r_s=4.00$ this calculation, Ekardt's calculation,[10] the variational calculation of Snider and Sorbello,[9] and the direct extrapolation of the plane metal surface results all give essentially the same answer for the static dipole polarizability of these jellium spheres—even for very small spheres containing only eight electrons. The enhancement of the polarizability over its classical value is seen to be directly proportional to the fraction of the electronic charge which extends beyond the positive background in the field-free system.

The results for $r_s=2.00$ show the same trends as those for $r_s=4.00$, however, in this system the quantum size effect due to the electronic orbitals is much more pronounced. This is not surprising, since the width of the occupied band is 0.39 a.u. for $r_s=2.00$ and 0.09 a.u. for $r_s=4.00$ ($N=92$), so the level spacing is much larger for these particles. The comparison with the variational calculation[9] indicates that a gradient expansion parameter of $\frac{1}{36}$ gives results in much better agreement with the quantum-mechanical calculations than those obtained using $\frac{1}{72}$.[18]

In order to further illustrate the effects of the electronic structure on the response of the sphere and the comparison with the response of a flat metal surface, the perturbed densities, $\delta n_1(r)$, for two neutral spheres ($r_s=2.00$) are shown in Fig. 3 (the arrows in this and subsequent figures indicate the centers of the spherical particles). These spheres contain $N=70$ and 92 electrons and their highest filled levels are $3s$ and $1g$, respectively (see Fig. 1). The density response for the flat metal surface computed by Lang and Kohn[14] is also shown in this figure. No adjustable parameters are involved in this comparison, since the correct normalization factor for their density can be obtained by noting that they require

$$\int_{-\infty}^{\infty} dz\,\delta n_p(z)=-1$$

and that the limiting expression, for $R\to\infty$, of the sum rule, Eq. (14), for neutral spheres is[19]

$$\frac{4\pi}{3}\int_{-\infty}^{\infty} dz\,\delta n_1(z+R)=-1\ .$$

The perturbed densities outside of the spheres, $r>R$, are remarkably similar, but nevertheless clearly reflect the variation in the values for δ and δ_p for these three cases. The other notable feature of the density response of these small spheres is the large amplitude of the response inside the sphere as compared to the response near the plane metal surface. This reflects in part the smaller amount of electronic charge density available to screen the field in this case; $(r/R)^2 n(r)$ for the spheres as compared to $n_p(z)$ for the flat surface. It also reflects the larger variations to be expected because the density is constructed from a small number of electron wave functions (this effect is also seen in the field-free calculations for spheres[5,6,20] and for thin films[21]). For spheres containing a larger number of electrons, these effects are less pronounced but they persist even for $N=254$ as shown in Fig. 4(b).

The radial component of the electric field is shown in Fig. 4(a). Also shown is the electric field near the surface of a classical metal sphere. Far outside the sphere this field strength behaves in the same manner as that for a classical metal sphere,

$$\epsilon_r(r,0)=\epsilon_0(1+2\alpha_1/r^3)\ . \qquad (18)$$

However, the electric field within the jellium sphere has an appreciable amplitude even at the center of the sphere. Also of note is the almost complete correspondence between the electric field outside the sphere here and in the variational calculation.[9]

A direct comparison of the results of this calculation with the model system RPA calculation of Rice *et al.*[11] for noninteracting electrons confined in a spherical well by an infinite potential barrier, is not meaningful, since it is quite clear that a very different definition of the sphere

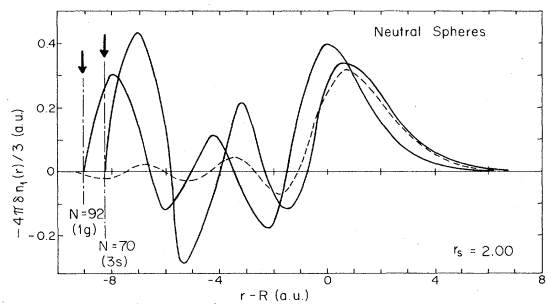

FIG. 3. Perturbed dipole density $4\pi\delta n_1(r)/3$ for neutral spheres with $r_s=2.00$ containing $N=70$ and 92 electrons. The dashed curve is the corresponding perturbed density $\delta n_p(z)$ for a plane surface, Ref. 14.

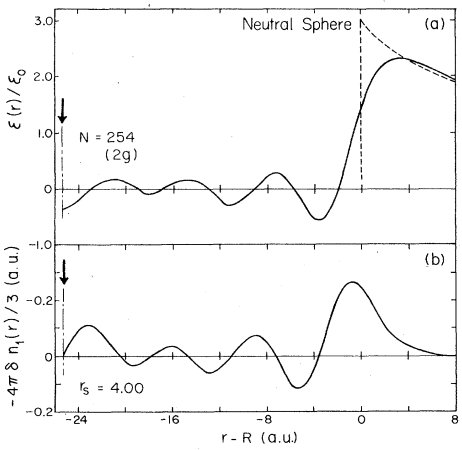

FIG. 4. Radial component of the electric field, $\epsilon(r)/\epsilon_0$, and the perturbed density $4\pi\delta n_1(r)/3$ for a neutral sphere with $r_s=4.00$. The dashed curve is the electric field for a classical metal sphere of the same radius.

radius was employed in that calculation. The only intrinsic length in their calculation is the radius of the well which is also the edge of the electronic charge distribution (this radius is also used to determine r_s or the density of the compensating positive charge). Hence, the electronic density goes to zero at the "surface" of their particle and the corresponding "classical" metal sphere has a constant electron density which extends up to this surface. An indication of what this model would give for δ, if the polarization was compared with a classical sphere with a more "reasonable" radius,[22] can be obtained by considering the infinite barrier model for a flat metal surface.[23,24]

For a flat metal surface one expects the electronic and ionic charge densities to be equal deep inside the metal and uses the charge neutrality of the system to locate the edge of the uniform positive density with respect to the infinite barrier [$d=3\pi/8k_F$, where $k_F=(3\pi^2 n_0)^{1/3}$]. For this model Newns[23] found

$$\delta_p \approx \left[\frac{\pi}{4k_F}\right]^{1/2} - \frac{\pi}{8k_F} = \begin{cases} 0.50 \text{ a.u.} & \text{for } r_s=2.00 \\ 0.46 \text{ a.u.} & \text{for } r_s=4.00 \end{cases}.$$

These values are positive, but much smaller than those obtained by Lang and Kohn.[14] Their smallness reflects the small amount of the electronic charge which extends outside of the positive background since the electrons cannot penetrate the region outside of the barrier.

The calculations for closed-shell configurations where the system (electrons and positive background) has one excess charge (total charge, $\pm e$) are reported in Fig. 5. These calculations reflect the expected features, since the principal effect in the field-free system is a raising or lowering of the effective potential $v_{\text{eff}}(r)$ for the single-particle states by[5] $\pm e^2/R$. For the positively charged system, this deepens the "well" seen by the electron and the electronic density response to the perturbing field is reduced. For the negatively charged system the reduction

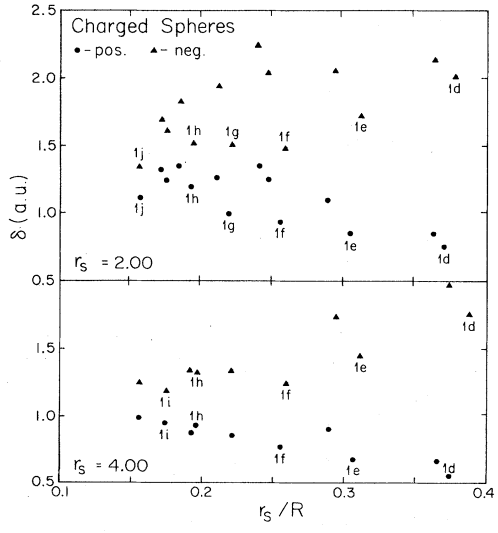

FIG. 5. Polarizability parameter δ for charged spheres with a charge $\pm e$. The data are for the same closed-shell configurations reported in Fig. 1 (only $1l$ points are labeled, but there is a one-to-one correspondence with the points in Fig. 1).

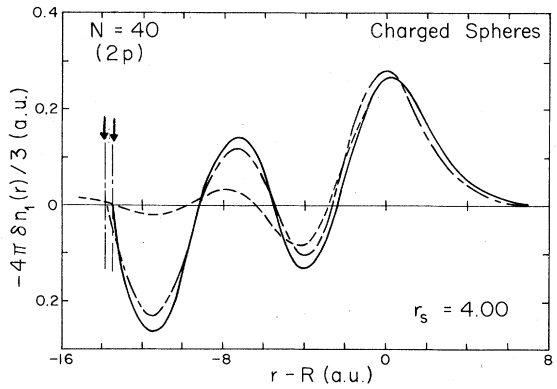

FIG. 6. Perturbed density $4\pi\delta n_1(r)/3$ for charged spheres with $r_s=4.00$ and $N=40$. The solid curve is for a sphere with a negative charge and the long-dash—short-dash curve for a sphere with a positive charge. The dashed curve is the corresponding perturbed density $\delta n_p(z)$ for a flat surface, Ref. 14 (this curve is not shown for $z=r-R>0$, since it falls between the other two curves in the figure).

of the well depth allows the electronic density to penetrate farther into the vacuum and there is a corresponding increase in the polarizability. The quantum size effect due to the electron orbitals is also larger for the negatively charged system.

In Fig. 6 the perturbed densities for two charged spheres with $r_s=4.00$ are plotted. Also shown is the density response for a flat surface[14] (outside of the sphere this density profile falls between those shown for the two charged spheres). Here, as for the neutral case, we can note the similarity of the responses outside of the spheres and the flat surface, and the large amplitude of the response interior to the sphere as compared to the flat surface.

IV. CONCLUSIONS

The quasiclassical calculations[9,25,26] and the quantum-mechanical calculations[5,6,27,10] of the work function and polarization[9,10] of small metal spheres which employ the jellium model provide a consistent picture of the electronic properties of these particles. The ionization potential and electron affinity are essentially identical for the field-free calculations when the effects of the shell structure, resulting from the high orbital degeneracy of the assumed spherical symmetry, are removed from the quantum-mechanical results.[5] The radial component of the electric field far outside of the sphere [Eq. (17)] depends on the polarizability of the sphere α_1 and the polarizability is well characterized by values of δ [Eq. (15)], which are essentially identical for the quasiclassical[25] and quantum-mechanical calculations.[5]

Our confidence in the consistency of the results obtained using the jellium model are further strengthened by the comparison of the self-consistent, quantum-mechanical calculations for small spheres[5] and the flat metal surface.[13,14] The field-free and perturbed density profiles [$n(r)$ and $\delta n_1(r)$, respectively] outside of the spherical positive charge density, $r>R$, and outside of the

flat surface are quantitatively the same (see Fig. 3, and Figs. 3 and 4 of Ref. 5). The ionization potential and electron affinity for the spheres converge, as they should, to the work function for the flat metal surface,[5] and the parameter δ is seen to converge to δ_p for the flat surface in an understandable fashion [Eq. (17)]. In fact, the quantitative agreement between $n(r)$ and $n_p(z)$, and the demonstrated proportionality of $\alpha_1/\alpha_{\rm cl}-1$ to $\Delta N/N$ (see Fig. 2) can easily be exploited to compute δ once δ_p and $n_p(z)$ are known for the flat surface.

The quantum size effect due to the electronic orbitals is quite pronounced when the polarization calculation for $r_s=2.00$ is displayed in terms of δ (Fig. 1). It is clear that these variations are principally due to the high orbital degeneracy inherent in the spherical symmetry of the model. For real metal clusters the lattice structure of the ionic charge will split these highly degenerate orbitals. Note, however, that the variations reported here have only a small effect on the polarization of the spheres.

A final point to be emphasized is that all of the density-functional calculations predict an enhancement of the polarizability of a jellium sphere over that for a classical metal sphere with the same radius as that of the uniform positive charge distribution. This result reflects the enhanced ability of the electronic charge, which "spills out" into the vacuum, to response to an applied field, and this enhancement should clearly be a feature of the experimental data for real metal clusters.

Note added. After the submission of this paper for publication, a Letter by Knight *et al.* [W. D. Knight, K. Clemenger, W. A. de Heer, W. A. Saunders, M. Y. Chou, and M. L. Cohen, Phys. Rev. Lett. **52**, 2141 (1984)] appeared reporting experimental results on the abundance of sodium clusters produced in a supersonic expansion. These authors conclude that the observed abundances are the result of the electronic structure provided by the conduction electrons bound in a spherically symmetric potential. This encourages the speculation that other effects due to these electronic orbitals may also be observable.

ACKNOWLEDGMENTS

The author has benefited greatly from many discussions with his colleagues Professor D. R. Snider and Professor R. S. Sorbello. In addition, I wish to thank Professor Sorbello for bringing the work in Ref. 2 to my attention.

APPENDIX A: MODIFIED STERNHEIMER EXPRESSION FOR THE POLARIZABILITY

Inserting the expansion (7) of $\delta n(\vec{r})$, into the expression (6) for $v_{\rm SCF}[\delta n;\vec{r}]$ and projecting out the Lth component, we obtain

$$v_L[\delta n;r]=r^M\delta_{L,M}+\frac{4\pi}{2L+1}\int dr'(r')^2\delta n_L(r')\frac{r_<^L}{r_>^{L+1}}+\delta n_L(r)\left[\frac{\partial^2}{\partial n^2}n\epsilon_{\rm xc}[n]\right]. \quad \text{(A1)}$$

Here we have used

$$|\vec{r}-\vec{r}'|^{-1}=\sum_{l,m}\frac{4\pi}{2l+1}Y_l^{*m}(\hat{r})Y_l^m(\hat{r}')\frac{r_<^l}{r_>^{l+1}}$$

and the orthogonality of the spherical harmonics. Equation (A1) is the central result of Mahan's proof,[2] since it demonstrates that the perturbing field will only couple to a density disturbance with the same symmetry. The restriction to spherically symmetric ground-state systems is embedded in the last term of this expression. If the ground-state density is not spherically symmetric (closed-shell configuration), then this last term will coupled $v_L[\delta n;r]$ to other density moments $\delta n_{L'}$, $L'\neq L$ and the perturbing field will produce density disturbances with additional moments.

To obtain the expression (11) for $\delta n_M(r)$, we need to expand $\delta n(\vec{r})$, $\psi_i(\vec{r})$, and $\phi_i(\vec{r})$ in spherical harmonics. Introducing

$$\phi_i(r)=\sum_{l',m'}r^{l'}w_{i,l'm'}(r)Y_{l'}^{m'}(\hat{r}),$$

where i represents the quantum numbers $(nlms)$, into the inhomogeneous differential equation for $\phi_i(\vec{r})$, (5), we can project out the $l''m''$ component

$$\sum_{l',m'}(L_{l'}-\epsilon_{nl})w_{i,l'm'}(r)\delta_{l'l''}\delta_{m'm''}=-v_M[\delta n;r]r^{l-l'}u_{nl}(r)\times\int d\Omega_{\hat{r}}Y_M^0(\hat{r})Y_l^m(\hat{r})Y_{l''}^{m''*}(\hat{r}). \quad \text{(A2)}$$

The integral over three spherical harmonics can be expressed in terms of Clebsch-Gordan coefficients[28] as

$$a^*(m;L;l,l'')=\int d\Omega_{\hat{r}}Y_l^m(\hat{r})Y_L^0(\hat{r})Y_{l''}^{m''*}(\hat{r})=\left[\frac{(2l+1)(2l'+1)}{4\pi(2l''+1)}\right]^{1/2}C(l,L,l'';m,0,m'')\times C(l,L,l'';0,0,0)$$

and

$$C(l,L,l'';m,0,m'')=\delta_{mm''}C(l,L,l'';m,0,m).$$

Therefore, the only nonzero components of $\phi_i(\vec{r})$ are those with $m'=m$.

Inserting the expansions for $\psi_i(\vec{r})$ and $\phi_i(\vec{r})$ into the expression (2) for $\delta n(\vec{r})$, and projecting out $\delta n_M(r)$, we find

$$\delta n_M(r)=4\,{\rm Re}\left[\sum_{n,l,m}r^l u_{nl}^*(r)\times\sum_{l'}r^{l'}w_{i,l'm}(r)a(m;M,l,l')\right]. \quad \text{(A3)}$$

Neither the operator nor the eigenvalue on the left-hand side of (A2) depends on $m=m'=m''$; therefore, we can multiply this equation by $a(m;M,l,l'')[c(M;l,l'')]^{-1}$ and sum over m to obtain the modified Sternheimer equation (12). We have introduced

$$\bar{u}_{nl,l'}(r)=[c(M;l,l')]^{-1}\sum_m w_{i,l'm}(r)a(m;M,l,l') \quad \text{(A4)}$$

and require

$$c(M;l,l')=\sum_m |a(m,M,l,l')|^2 . \quad \text{(A5)}$$

Substituting $\bar{u}_{nl,l'}(r)$ into (A3) gives (11).

Evaluating (A5) for $M=1$, we obtain[2]

$$c(1;l,l')=(l+1)\delta_{l',l+1}+l\delta_{l',l-1} .$$

APPENDIX B: NUMERICAL PROCEDURES

In order to facilitate the numerical solution of the differential equations for $u_{nl}(r)$ and $\bar{u}_{nl,l'}(r)$, Eqs. (9) and (12), respectively, it is useful to factor out the dominate behavior of these functions for large and small r. For small r, $v_{\rm eff}[n;r]\approx$const and one easily finds that $u_{nl}(r)\propto$const. For large r, $v_{\rm eff}[n;r]\approx 0$ and $u_{nl}(r)\propto r^{-(l+1)}\exp(-ar)$, where $a=(-2\epsilon_{nl})^{1/2}$. The eigenvalues ϵ_{nl} are to be determined by the numerical procedure, so they cannot be used in the factorization. We use instead $a=(-2\epsilon'_{\rm max})^{1/2}$, where $\epsilon'_{\rm max}$ is the energy of the highest filled level in the preceding iteration. Hence, we can account for the dominant behavior of $u_{nl}(r)$ by setting

$$u_{nl}(r)=f_{nl}(r)\left[1+\left[\frac{r}{R}\right]^2 e^{a_l(r-R)}\right]^{-(l+1)/2} ,$$

where $a_l=2a/(l+1)$. Commuting the explicit factor through L_l, we obtain

$$L_l^{\rm eff} f_{nl}(r)=\epsilon_{nl} f_{nl}(r) , \quad \text{(B1)}$$

where $L_l^{\rm eff}$ is defined so that

$$L_l u_{nl}(r)=\left[1+\left[\frac{r}{R}\right]^2 e^{a_l(r-R)}\right]^{-(l+1)/2} L_l^{\rm eff} f_{nl}(r) .$$

For large r, the right-hand side of (12) is given by $r^{l-l'+M}u_{nl}(r)$, since $v_M[\delta n;r]\approx r^M$. Inside the particle the perturbing field will be partially screened by the electrons, but the dominant behavior should still be given by the variation in $u_{nl}(r)$. Hence, we use the factorization $\bar{u}_{nl,l'}(r)=g_{nl,l'}(r)u_{nl}(r)$ to account for the dominant behavior of $\bar{u}_{nl,l'}(r)$. With this factorization we can replace (12) by

$$K^{\rm eff}_{nl,l'}g_{nl,l'}(r)=-r^{l-l'}v_M[\delta n;r] , \quad \text{(B2)}$$

where $K^{\rm eff}_{nl,l'}$ is defined by

$$(L_{l'}-\epsilon_{nl})\bar{u}_{nl,l'}(r)=u_{nl}(r)K^{\rm eff}_{nl,l'}g_{nl,l'}(r) .$$

The second-order differential equations (B1) and (B2) are solved by introducing a set of quadrature points r_j and evaluating the first and second derivatives by using finite differences. Thus the function $f_{nl}(r)[g_{nl,l'}]$ evaluated at the points $r=r_j$ are the components of a column vector and $L_l^{\rm eff}[K^{\rm eff}_{nl,l'}]$ is replaced by a matrix with components $\mathscr{L}_{ij}(k_{ij})$. These procedures convert the differential equations into matrix equations which can be solved by standard numerical programs. The effect of the factorizations described above is to balance the components of the column vectors; i.e., the components $f_{nl}(r_j)[g_{nl,l'}(r_j)]$ are all the same order of magnitude, but the wave function $u_{nl}(r)[\bar{u}_{nl,l'}(r)]$ will vary over many orders of magnitude as r is varied.

The solution of (B1) for the eigenvectors $f_{nl}(r_j)$ and the eigenvalues ϵ_{nl} determine $u_{nl}(r)$. The matrix inverse[29] of $K^{\rm eff}_{nl,l'}$, components k_{ij}^{-1}, is used to determine

$$\bar{u}_{nl,l'}(r_i)=-u_{nl}(r_i)\sum_j k_{ij}^{-1}r_j^{l-l'}v_M[\delta n;r_j] .$$

Inserting this expression into (11), we obtain

$$\delta n_M(r_i)=-\sum_j m_{ij}v_M[\delta n;r_j] ,$$

where the matrix elements m_{ij} are given by

$$m_{ij}=4\,{\rm Re}\left[\sum_{n,l,l'} r^{l+l'}|u_{nl}(r_i)|^2 k_{ij}^{-1}c(M;l,l')\right] .$$

The self-consistent density response δn_M can then be determined by iterative solution of this matrix equation in combination with the expression (8) for $v_M[\delta n;r]$.

[1] M. J. Scott and E. Zaremba, Phys. Rev. A **21**, 12 (1980); A. Zangwill and P. Soven, Phys. Rev. A **21**, 1561 (1980).

[2] G. D. Mahan, Phys. Rev. A **22**, 1780 (1980).

[3] G. D. Mahan, Solid State Commun. **33**, 797 (1980); Solid State Ionics **1**, 29 (1980).

[4] R. M. Sternheimer, Phys. Rev. **96**, 951 (1954); **107**, 1565 (1957).

[5] D. E. Beck, Solid State Commun. **49**, 381 (1984).

[6] W. Ekardt, Phys. Rev. B **29**, 1558 (1984).

[7] P. Hohenberg and W. Kohn, Phys. Rev. **136**, B864 (1964).

[8] W. Kohn and L. J. Sham, Phys. Rev. **140**, A1133 (1965); N. D. Lang, in *Solid State Physics,* edited by H. Ehrenreich, F. Seitz, and D. Turnbull (Academic, New York, 1973), Vol. 28, p. 225.

[9] D. R. Snider and R. Sorbello, Phys. Rev. B **28**, 5702 (1983).

[10] W. Ekardt in *Berichte des Bunsen-Gesellschaft: Conference Proceedings of the International Discussion Meeting "Experiments on Clusters" Koenijstein, 1983* (in press); W. Ekardt, Phys. Rev. Lett. **52**, 1925 (1984). While the calculations reported in this paper were being carried out, we received from Dr. Ekardt prepublication reports on his results.

[11] M. J. Rice, W. R. Schneider, and S. Strässler, Phys. Rev. B **8**, 474 (1973).

[12] Other references to RPA calculations for an electron confined by an infinite potential barrier: L. P. Gor'kov and G. M. Eliashberg, Zh. Eksp. Teor. Fiz. **48**, 1407 (1965) [Sov. Phys.—JETP **21**, 940 (1965)]; A. Kawabatta and R. Kubo, J. Phys. Soc. Jpn. **21**, 1765 (1966); A. A. Lushikov and A. J. Simonov, Phys. Lett. **44A**, 45 (1973); M. Cini and P. Ascarelli, J. Phys. F **4**, 1998 (1974). Recent references: A. A. Lushikov, V. V. Maksinenko, and A. J. Simonov, in *Electromagnetic Surface Modes,* edited by A. D. Boardman (Wiley, New York, 1982); D. M. Wood and N. W. Ashcroft, Phys. Rev. B **25**, 6255 (1982).

[13] N. D. Lang and W. Kohn, Phys. Rev. B **3**, 1215 (1971); **1**,

4555 (1970).
[14]N. D. Lang and W. Kohn, Phys. Rev. B **7**, 3541 (1973).
[15]R. S. Sorbello, Solid State Commun. **48**, 989 (1983).
[16]R. S. Sorbello (private communication).
[17]In the calculations reported here the sum rule is satisfied with an error of $\pm 0.2\%$.
[18]This conclusion was also reported in Ref. 9.
[19]This requires that integrals of the form $R^{-n}\int_{-R}^{0} dr\, r^n \delta n_1(r+R)$ vanish as $R\to\infty$. This has been demonstrated by Lang and Kohn, Ref. 13.
[20]A. Hintermann and M. Manninen, Phys. Rev. B **27**, 7262 (1983).
[21]F. K. Schulte, Surf. Sci. **55**, 427 (1976).
[22]This is of course the same effect as that produced by Cini's rescaling of the size of the spherical well [M. Cini, J. Opt. Soc. Am. **71**, 386 (1981)].
[23]D. M. Newns, Phys. Rev. B **1**, 3304 (1970).
[24]D. E. Beck and V. Celli, Phys. Rev. B **2**, 2955 (1970).
[25]D. R. Snider and R. S. Sorbello, Solid State Commun. **47**, 845 (1983).
[26]M. P. Iniguez, C. Baladron, and J. A. Alonso, Surf. Sci. **127**, 367 (1983); M. Cini, J. Catalysis **37**, 187 (1975).
[27]J. L. Martins, R. Car, and J. Buttet, Surf. Sci. **106**, 265 (1981).
[28]These are Gaunt coefficients. See E. U. Condon and G. H. Shortley, *The Theory of Atomic Spectra* (Cambridge University Press, London, 1963), pp. 178 and 179, or M. Tinkham, *Group Theory and Quantum Mechanics* (McGraw-Hill, New York, 1964), Appendix C, for tables of these coefficients.
[29]This procedure fails if ϵ_{nl} is also an eigenvalue of $L_{l'}$, $(l'\neq l)$. This corresponds to a degeneracy in the solution of the field-free problem, which must be removed, just as in the calculation of the first-order Stark effect for an excited state of the hydrogen atom.